The 7th International Conference on Discrete Element Methods
August 1 to August 4, 2016
Dalian, China

Numerical Investigation of Optical Sorting using the Discrete Element Method

C. Pieper, H. Kruggel-Emden[1], S. Wirtz, V. Scherer, F. Pfaff, B. Noack, U.D. Hanebeck, G. Maier, R. Gruna, T. Längle, J. Beyerer

Abstract. Automated optical sorting systems are important devices in the growing field of bulk solids handling. The initial sorter calibration and the precise optical sorting of many materials is still very time consuming and difficult. A numerical model of an automated optical belt sorter is presented in this study. The sorter and particle interaction is described with the Discrete Element Method (DEM) while the separation phase is considered in a post processing step. Different operating parameters and their influence on sorting quality are investigated. In addition, two models for detecting and predicting the particle movement between the detection point and the separation step are presented and compared, namely a conventional line scan camera model and a new approach combining an area scan camera model with particle tracking.

Keywords: Bulk solids handling; Discrete Element Method (DEM); optical sorting; non-spherical particles; multiple object tracking

1. Introduction

With continuously growing material streams the handling and sorting of bulk solids is of great importance [1]. Apart from conventional separating processes like screens [2], which separate the material depending on physical properties, automated optical sorters can be used. Bulk solids from different industries like agricultural products or particulate chemical/pharmaceutical substances can be separated based on optical criteria [3]. The particulate matter is transported and isolated by chutes, slides or vibrating feeders and passed by an optical sensor. The bulk solids are then separated into two fractions by pneumatic air valves, which are triggered based on optical properties of the material.

[1] H. Kruggel-Emden (✉)
Ruhr-University Bochum, Universitaetsstrasse 150, 44780 Bochum, Germany
e-mail: kruggel-emden@leat.rub.de

Studies investigating the influence of optical sorter design and operation on sorting quality are relatively scarce. In 2005 De Jong and Harbeck [4] investigated the maximum throughput of an optical sorter based on different particle sizes. They concluded that the separation efficiency decreases if a minimum distance between adjacent particles is below a certain threshold. Pascoe et al. [5] developed a model for predicting the efficiency of their sorting system depending on the belt loading and the amount of particles to be ejected. In a further study [6] the authors investigated the influence of particle distribution on sorting efficiency with the help of a Monte Carlo simulation. Particle ejection by compressed air has been investigated with a coupled DEM-CFD approach by Fitzpatrick et al. [7].

In this study an optical belt sorter is modeled with the DEM and the influence of different operating parameters on sorting quality are investigated. In addition, the results of employing a model of a standard optical line scan camera (thereby assuming that the particles are moving in belt direction with belt velocity at the detection point) are compared to using the model of an area scan camera with combined particle tracking (the actual particle velocity and direction of movement at the detection point are considered). A detailed description of the process can be found in [8, 9]. Particle ejection is represented as a post processing step.

2. Methodology

The optical belt sorter and the bulk solids investigated in this study are described with the Discrete Element Method (DEM) [10]. It allows the detailed analysis of particle-particle and particle-wall interactions. The translational and rotational motion of every particle is calculated with Newton's and Euler's equations of motion and can be written as

$$m_i \frac{d^2\vec{x}_i}{dt^2} = \vec{F}_i^c + \vec{F}_i^g, \tag{1}$$

$$\hat{I}_i \frac{d\vec{W}_i}{dt} + \vec{W}_i \times \left(\hat{I}_i \vec{W}_i\right) = \Lambda_i^{-1} \vec{M}_i, \tag{2}$$

where m_i is the particle mass, $d^2\vec{x}_i/dt^2$ the particle acceleration, $\vec{F}_i^c$ the contact force and $\vec{F}_i^g$ is the gravitational force. The second equation gives the angular acceleration $d\vec{W}_i/dt$ as a function of the angular velocity $\vec{W}_i$, the external moment resulting out of contact forces $\vec{M}_i$, the inertia tensor along the principal axis $\hat{I}_i$ and the rotation matrix converting a vector from the inertial into the body fixed frame Λ_i^{-1}. The utilized contact forces as well as the applied rolling friction model are presented in [11]. The non-spherical particles employed in this study are modeled with polyhedrons, while the contact detection is based on a fast common plane algorithm [12]. The contact force laws are equal to those of spherical particles [13, 14].

3. Numerical Setup and Simulation Parameters

The numerically modelled optical belt sorter is based on a fully functional miniaturized sorting system. A sketch of the sorter and its main components is presented in Fig. 3.1. In all conducted simulations the conveyor belt runs at a constant velocity of 1.5 ms^{-1} and equal portions of red and blue particles are to be separated.

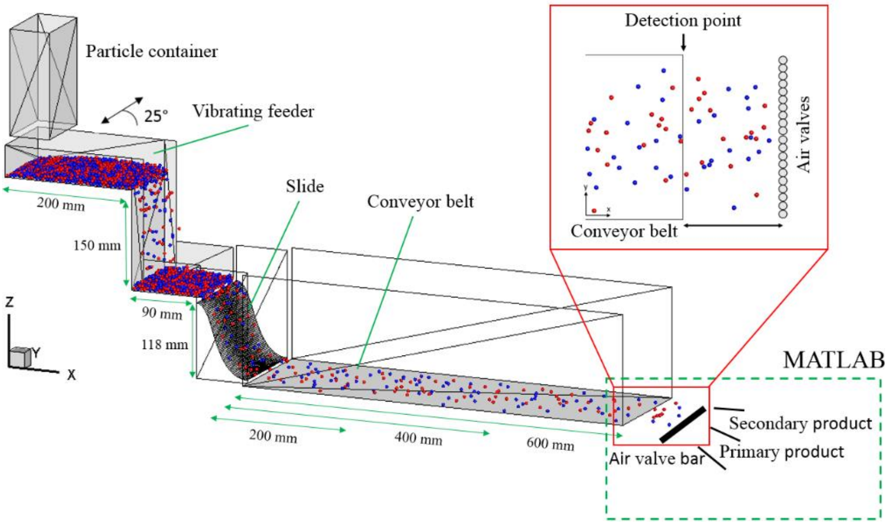

Fig. 3.1 Schematic of the optical belt sorter

The separation phase of the system (dashed box in Fig. 3.1) is represented by a MATLAB script based on particle information generated with the DEM. A certain number of air valves are assumed to be located in a straight line at a predefined distance to the end of the conveyor belt (see Fig. 3.1). Two models for predicting the particle movement between the detection point at the end of the belt and the valve bar are employed. In the first model the particles are assumed to move at belt velocity without any cross movements and a conventional line scan camera is used for particle detection. In the second model the x- and y-velocities of the particles at the detection point are considered. This is possible due to a more sophisticated approach combining an area scan camera with particle tracking [8, 9].

The material parameters of the employed particle shapes are based on beech wood particles [15]. The coefficients of restitution as well as Coulomb and rolling friction were determined experimentally according to procedures outlined in [16]. The initial particle packing within the particle container is generated randomly.

To compare the impact of the two prediction models and different operating parameters on the separation efficiency of the optical sorter, a base case is defined and six operating parameters are altered one at a time in multiple simulation series. The conducted investigations are presented in Table 3.1. The highlighted values represent the base case of the study. The DEM simulations are conducted with a time step of $1 \cdot 10^{-5}$ s.

Table 3.1 Operational system parameters investigated on the MATLAB and DEM side

MATLAB (Valves)						Discrete Element Method		
Quantity [-]		Activation duration [s]		Bar distance [m]		Applied particle mass [kg]	Conveyor belt length [m]	Particle shape [-]
12	28	0.0025	0.01	0.03	0.09	0.1	0.2	Cylinders
16	32	0.004	0.015	0.05	0.10	0.2	0.4	Spheres
20	36	0.005	0.02	0.07	0.11	0.3	0.6	Plates
24	40							

4. Results and Discussion

To assess the separation quality of the sorter, two indicators are analysed for each simulation series. The first is the percentage of particles not ejected by the air valves although they should have been separated from the material stream and the second is the number of falsely co-ejected particles. Particles are considered as ejected if their centre of gravity is within the valve radius (see Fig. 3.1) during the activation time of the valve. For a clear visual presentation, the curves of the not ejected particle models are represented by dashed lines and those of the falsely ejected particle models with solid ones.

4.1 Influence of Valve Parameters

The percentages of not ejected and falsely co-ejected particles are outlined for different valve parameters in Fig. 4.1.

The first investigated parameter is the number of employed air valves. The results are presented in Fig. 4.1a. The graph shows that the percentage of not ejected particles continuously increases with rising air valve numbers for both prediction models. The percentage of falsely co-ejected particles decreases with rising valve numbers. This was expected, as the air influence radius is significantly reduced when employing higher numbers of air valves on the same belt width. The number of not ejected particles, when assuming perfect separation based on exact particle positions at the separation point, are obviously zero at all times. Significantly more particles are not ejected when applying the line scan camera compared to the area scan camera model. The difference between the models regarding falsely co-ejected particles is only very marginal in comparison.

The findings of employing different valve activation durations are depicted in Fig. 4.1b. The figure shows that the percentage of not ejected particles is considerably higher when employing the line scan camera instead of the area scan camera model, especially at low activation durations. During the very short air blast intervals of 0.0025s to 0.004s only a precise prediction of the x-velocity ensures a good separation quality. The number of falsely co-ejected particles of both models increases almost linearly with rising valve activation duration.

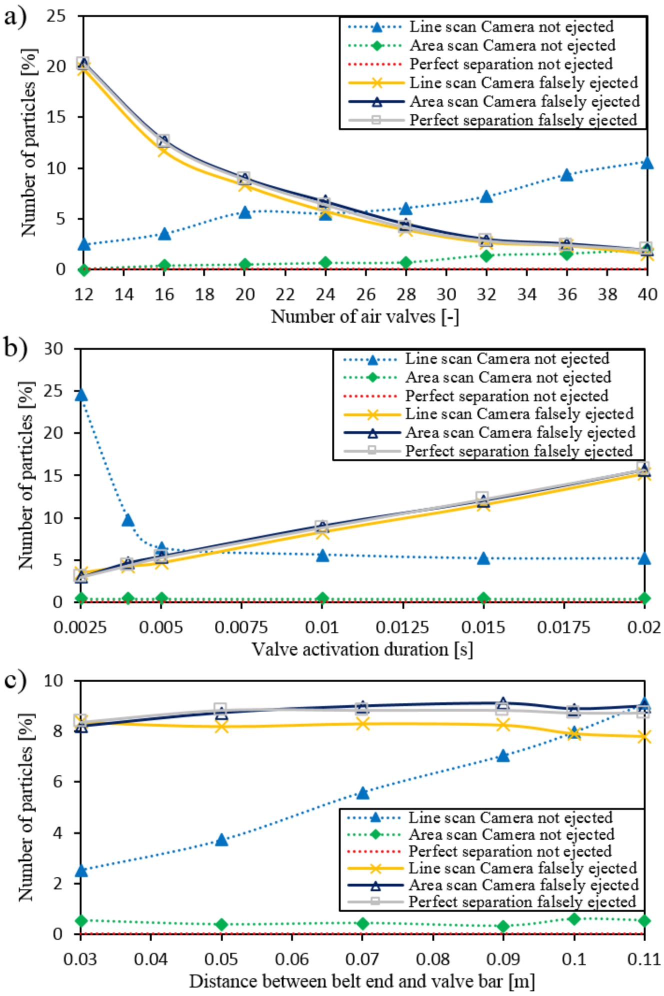

Fig. 4.1 Influence of the a) number of air valves, b) valve activation duration and c) distance between belt end and valve bar on the separation quality

The third investigated parameter is the distance between the belt end and the valve bar. The results are presented in Fig. 4.1c. The percentage of not ejected particles increases linearly for the line scan camera model with a rising gap between detection and separation point. In contrast, the number of not ejected particles, when employing the area scan camera model, is significantly lower and remains almost constant. The percentage of falsely co-ejected particles also seems to be relatively independent of the distance between the detection and separation stage.

4.2 Influence of Simulation Parameters

The percentages of not ejected and falsely co-ejected particles for different simulation parameters are presented in Fig. 4.2.

Fig. 4.2a shows the influence of different conveyor belt lengths on separation quality. At short belt lengths, the percentage of not ejected particles is very high when applying the line scan camera model, as it is falsely assumed that the particles have already reached belt velocity and orthogonal movement to the belt direction is still high. With increasing belt length this percentage drastically decreases. When applying the area scan camera model combined with particle tracking, the number of not ejected particles remains at a constant low value. The amount of falsely co-ejected particles also seems unaffected by belt length.

The impact of different applied particle masses is presented in Fig. 4.2b. The graph shows that the percentages of not ejected and falsely co-ejected particles increase for all investigated models with rising applied particle masses. A higher throughput causes increased particle interaction and proximity leading to a higher likelihood of irregular particle movement and false co-ejection. Again, the area scan camera model combined with particle tracking shows a better separation quality compared to the line scan camera model.

The final investigated simulation parameter is the particle shape. The results are shown in Fig. 4.2c. It can be seen that the percentages of particles not ejected by the air valves are very similar for cylinders and spheres but considerably lower for plates. In contrast to the other two shapes, plates develop no rolling motion once they enter the conveyor belt, resulting in considerably less cross movement. Due to this they also adapt to the belt velocity at a much quicker rate. The percentages of not ejected particles based on the area scan camera model are considerably lower for all investigated shapes. The number of falsely co-ejected particles is highest for cylinders, followed by plates and lastly spheres. The employed particle shapes are not transported evenly by the vibrating feeder leading to differences in particle feed rate and therefore particle proximity on the conveyor belt. As previously discussed, higher particle proximity increases the likelihood of false co-ejection.

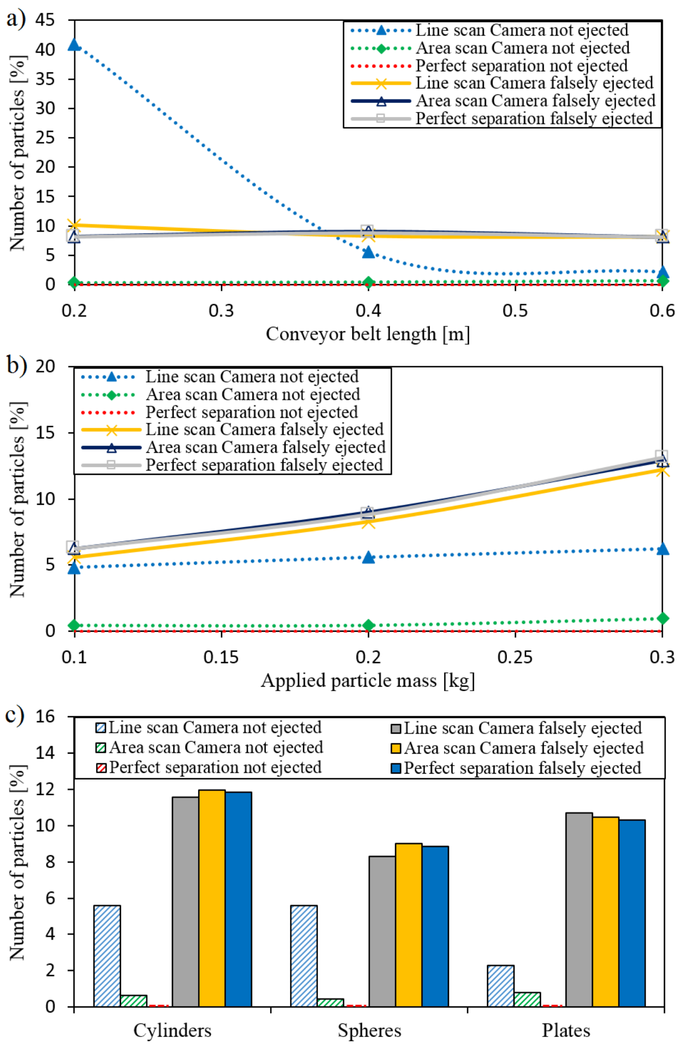

Fig. 4.2 Influence of the a) conveyor belt length, b) applied particle mass and c) particle shape on the separation quality

5. Conclusions

In this study an automated optical belt sorter was numerically modelled with the DEM and the influences of two particle movement prediction models and different operating parameters on sorting quality were assessed.

The model of the area scan camera combined with particle tracking is superior to the line scan camera approach in all investigated operation modes. Detailed knowledge of particle motion and behaviour greatly enhances the separation quality of optical sorters.

The investigation showed that plausible results regarding the influence of different operating parameters on sorting quality can be obtained with numerical simulations. Obtained information can be utilized for sorter calibration and optimization.

Further and more detailed studies will include the coupling of DEM with Computational Fluid Dynamics (CFD) to accurately describe the separation phase with compress air and the modelling of industrial bulk solids like coffee beans, glass shards or peppercorns.

6. References

1. Duran J (2000) Sands, Powders and Grains, Springer New York, New York
2. Stieß M (1995) Mechanische Verfahrenstechnik 1, Springer Berlin Heiderlberg, Berlin
3. McGlichey D (2005) Characterisation of Bulk Solids, Blackwell Publishing Ltd., Oxford
4. De Jong, Harbeck TPR. (2005) Automated sorting of minerals: current status and future outlook. In: Proc. 37th Can. Miner. Process. Conf. 629-648
5. Pascoe RD, Udoudo OB, Glass HJ (2010) Efficiency of automated sorter performance based on particle proximity information. In: Miner. Eng. 23 806-812
6. Pascoe RD, Fitzpatrick R, Garratt JR (2015) Prediction of automated sorter performance utilizing a Monte Carlo simulation of feed characteristics. In: Miner. Eng. 72 101-107
7. Fitzpatrick RS, Glass HJ, Pascoe RD (2015) CFD-DEM modelling of particle ejection by a sensor-based automated sorter. In: Miner. Eng. 79 176-184
8. Pfaff F, Baum M, Noack B, Hanebeck UD, Gruna R, Laengle T et al. (2015) TrackSort: Predictive tracking for sorting uncooperative bulk materials. IEEE Int. Conf. Multisens. Fusion Intergr. Intell. Syst. 2015
9. Pfaff F, Pieper C, Maier G et al. (2016) Improving optical sorting of bulk materials using sophisticated motion models. In: tm – Technisches Messen. 83 77-84
10. Cundall, PA, Strack ODL (1979) A discrete numerical model for granular assemblies. In: Geotechnique. 29 47-65
11. Sudbrock F, Simsek E, Rickelt S, Wirtz S, Scherer V (2011) Discrete element analysis of experiments on mixing and stoking of monodisperse spheres on a grate. In: Powder Technol. 208 111-120
12. Höhner D (2014) Experimentelle und numerische Untersuchungen zum Einfluss von Partikelgeometrie auf das mechanische Verhalten von Schüttgütern mit Hilfe der Diskreten Elemente Methode
13. Kruggel-Emden H, Simsek E, Rickelt S, Wirtz S, Scherer V (2007) Review and extension of normal force models for the Discrete Element Method. In: Powder Technol. 171 157-173
14. Kruggel-Emden H, Wirtz S, Scherer V (2007) An analytical solution of different configurations of the linear viscoelastic normal and frictional-elastic tangential contact model. In: Chem. Eng. Sci. 62 6914-6926
15. Vollmari K, Jasevicius R, Kruggel-Emden H (2016) Experimental and numerical study of fluidization and pressure drop of spherical and non-spherical particles in a model scale fluidized bed. In: Powder Technol. 291 506-521
16. Höhner D, Wirtz S, Scherer V (2013) Experimental and numerical investigation on the influence of particle shape and shape approximation on hopper discharge using the discrete element method. In: Powder Technol. 235 614-627